

# Chemical vapor detection using single-walled carbon nanotubes†

E. S. Snow, F. K. Perkins and J. A. Robinson

Received 7th April 2006

First published as an Advance Article on the web 24th May 2006

DOI: 10.1039/b515473c

Single-walled carbon nanotubes possess unique properties that make them a potentially ideal material for chemical sensing. However, their extremely small size also presents technical challenges for realizing a practical sensor technology. In this *tutorial review* we explore the transduction physics by which the presence of molecular adsorbates is converted into a measurable electronic signal, and we identify solutions to the problems such as nanotube device fabrication and large, low-frequency noise that have inhibited commercial sensor development. Finally, we examine strategies to provide the necessary chemical specificity to realize a nanotube-based detection system for trace-level chemical vapor detection.

Naval Research Laboratory, Washington, DC 20375, USA

† The HTML version of this article has been enhanced with colour images.



Eric S. Snow

Eric S. Snow is Head of the Nanotechnology Section at the Naval Research Laboratory (NRL) in Washington, DC. Dr Snow received his PhD in Physics from the University of North Carolina at Chapel Hill in 1986. He has been a member of the full-time research staff at NRL since 1987. The Nanotechnology Section specializes in nanoscale materials and the MBE-growth of the InAs/GaSb/AlSb semiconductor family. Research on these materials ranges from basic

materials studies to device development in the areas of chemical sensors, high-speed electronics and IR detectors/lasers.



F. Keith Perkins

Keith Perkins earned a BS degree in Physics from MIT in 1982, and an MS and PhD in Materials Science from the University of Wisconsin-Madison in 1987 and 1992, respectively. He was awarded a National Research Council fellowship, tenured at the Naval Research Laboratory, Washington DC, in 1992. He became an NRL employee in 1995. He has authored or co-authored over 40 papers in refereed journals, and is a co-inventor on 6 patents or disclosures.



Joshua A. Robinson

Joshua A. Robinson earned a BS from Towson University in 2001 and subsequently studied at Penn State University as a NDSEG Graduate Fellow, earning his PhD in 2005. He was awarded a National Research Council Post-doctoral Fellowship in 2005 to study at the Naval Research Laboratory under the direction of Dr Snow. Dr Robinson's research focus is on the physics and chemical specificity of SWNT chemical sensors.

## 1. Introduction

Single-wall carbon nanotubes (SWNTs) are cylinders of graphite  $\sim 1$  nm in diameter,  $\sim 1$   $\mu\text{m}$  long, and with a wall thickness of one atomic layer. This unique structure results in electronic and chemical properties that are ideal for the direct electronic detection of trace chemical vapors. Because SWNTs are composed entirely of surface atoms, molecular adsorbates can significantly alter their electronic properties.<sup>1,2</sup> SWNTs also exhibit near-ballistic electron transport along the tube axis,<sup>3</sup> which provides a high-quality electrical conduit for transmission of such electrical perturbations to external contacts. Finally, the graphitic surface of SWNTs is chemically robust, allowing long-term stable operation.

This unique combination of properties has motivated researchers to pursue the development of a SWNT sensor technology. Initial work by Kong, *et al.*<sup>1</sup> and Collins *et al.*<sup>2</sup> demonstrated that the conductance of SWNTs changes in response to exposure to certain molecules that undergo charge transfer upon adsorption. The sensitivity to both electron donating ( $\text{NH}_3$ ) and withdrawing ( $\text{NO}_2$ ) molecules was found to be superior to commercial sensors with 100-part-per-trillion sensitivity demonstrated for  $\text{NO}_2$ .<sup>4</sup>

In addition to this conductance-based detection scheme, we have developed a capacitance-based sensor that detects the polarization of molecular adsorbates. We find that dilute concentrations of a wide range of chemical vapors produce a rapid, reversible change in capacitance.<sup>5</sup>

Researchers have used both conductance and capacitance-based SWNT sensors to detect a wide variety of chemical vapors and gases including simulants for chemical warfare agents and explosives,<sup>5–7</sup> toxic chemicals,<sup>4</sup> and as a detector for medical breath analysis.<sup>8</sup> These initial laboratory demonstrations provide sufficient promise to justify further development of a SWNT-based chemical sensor technology.

In order to progress from laboratory demonstration to commercial sensor technology significant scientific and technological challenges must be addressed. These challenges include reliable nanotube device fabrication, an inherently high level of  $1/f$  noise, and achieving chemical specificity. Recently, researchers have developed approaches to address each of these problems and significant progress has been made toward a practical sensor technology.

In this tutorial we examine the current state of development of SWNT-based chemical sensors. The first topic we address is SWNT-based device fabrication. Inexpensive, high-yield fabrication is essential to the success of SWNT sensor technology. As a way to circumvent the difficult process of precise assembly of SWNTs, we discuss the use of SWNT networks that contain a large number of randomly positioned nanotubes.<sup>9</sup> Sensors fabricated from such networks average the properties of many individual SWNTs and can be fabricated with high yield using conventional microfabrication techniques.

We next explore the topic of signal transduction, the process of converting the presence of chemical adsorbates into a measurable electrical response. We examine both conductance- and capacitance-based modes of detection. These two detection modes provide complementary capabilities and information.<sup>10</sup> It should be noted that this tutorial is confined to the discussion of chemical vapor detection. SWNTs also show promise as electrochemical sensors for chemical or biological detection. We have chosen to concentrate on vapor detection, because in this area SWNTs offer unique performance that cannot be achieved using conventional solid-state sensors.

A critical issue for maximizing the performance of SWNT sensors is electrical noise reduction. Unfortunately, SWNTs, as well as other nanoscale materials, exhibit a large component of  $1/f$  noise.<sup>11</sup> Such  $1/f$  noise is a particular concern for chemical detection, because the sensors operate at low frequencies. We discuss how SWNT networks can be designed to reduce the level of  $1/f$  noise to acceptable levels.<sup>12</sup>

Lastly, we discuss the issue of chemical specificity. One approach to chemical specificity is to apply molecular coatings on the SWNTs to selectively amplify or filter the response to a particular analyte or class of chemical.<sup>4–6,10</sup> Additionally, the fast response time of SWNT sensors is compatible with newly developed micro gas chromatographs that temporally separate the target vapor from potential interferents. Research in this area is ongoing and critical to the future success of SWNT sensor technology.

These topic areas of sensor fabrication, signal transduction, noise reduction, and chemical specificity represent the four

main research thrusts of SWNT sensor development. These issues are not unique to SWNTs, but are common to many potential sensor technologies based on nanoscale electronic materials. Consequently, the approaches taken for SWNT sensor development can serve as a guide for other nanoscale sensor technologies as well.

## 2. High-yield sensor fabrication

Commercialization of SWNT devices and sensors has been impeded by failure to develop a high-yield manufacturing process. Such high-yield fabrication is difficult because currently no reliable method exists for precisely positioning and orienting individual SWNTs. In addition, available growth techniques produce SWNTs with different chiralities and diameters, which result in electronic properties ranging from metallic to semiconducting.<sup>13</sup> Consequently, the properties of SWNT devices will depend on the position, number and electronic type of its constituent nanotubes and none of these parameters can currently be controlled with a high degree of reproducibility.

### SWNT networks

One solution to the manufacturing problem is to construct devices using two-dimensional networks of SWNTs.<sup>9</sup> These networks consist of an intersecting two-dimensional random array of SWNTs that are either grown or deposited from solution onto a substrate (Fig. 1). If the average distance between SWNTs is less than the average nanotube length, then the SWNTs will form an interconnected network that is electrically continuous over macroscopic dimensions. The

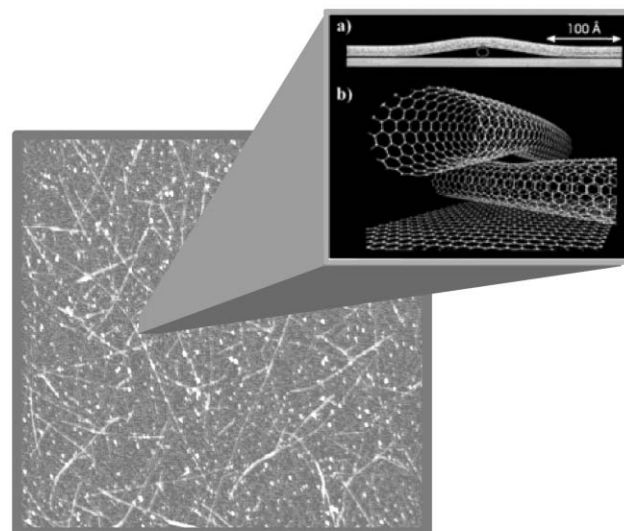


**Fig. 1** A  $5 \times 5 \mu\text{m}^2$  atomic-force-microscope image of a SWNT network. With our growth conditions the average nanotube diameter is about 1.2 nm, lengths range from about 1 to 5  $\mu\text{m}$ , and the density ranges from 3 to 10 SWNTs per  $\mu\text{m}^2$ . The nanotubes cover about 1% of the total surface area of the substrate. The inset shows the results of molecular-mechanical calculations of intersecting SWNTs. (Reproduced with permission from Ref. 14. Copyright 1998 The American Physical Society.)

electronic properties of such networks reflect the aggregate behavior of many randomly positioned SWNTs.

Such random networks can be used to circumvent the assembly issues with SWNTs and achieve high-yield sensor fabrication. SWNT networks are compatible with conventional semiconductor microfabrication techniques, and uniform sensor properties are achieved provided the devices incorporate a sufficiently large number of SWNTs. In the future it may be possible to construct devices with SWNTs that are of uniform chirality and that are precisely aligned, and such devices might provide superior sensor properties. However, a practical SWNT assembly process will have to maintain the low cost and high yield of random SWNT networks.

Key to the electronic quality of random networks is the electrical contact that is formed between intersecting SWNTs lying on a surface. SWNTs adhere to surfaces such as SiO<sub>2</sub> via van der Waals forces.<sup>14</sup> Because SWNTs are extremely stiff (Young's modulus  $\sim 10^{12}$  Pa),<sup>15</sup> when two SWNTs cross the van der Waals force pulling down on the top SWNT is transferred to the point of intersection. This force is sufficient to deform the two SWNTs at the point of intersection and pulls them closer together than the interplane spacing in graphite (see inset Fig. 1). This close contact increases the inter-nanotube tunneling probability, which in certain cases can be as high as  $0.1 e^2/h$  (where  $4 e^2/h$  is the ideal ballistic conductance of a SWNT<sup>16</sup>). These inter-nanotube point contacts create an electrically continuous network over arbitrarily large dimensions, provided that the level of interconnectivity exceeds the threshold for conductivity.

### Growth and fabrication

The details of SWNT growth and device fabrication can be found in the literature (*e.g.* Ref. 9). Briefly, the sensors consist of microfabricated metal electrodes deposited on electrically continuous two-dimensional networks of SWNTs. The network is often grown on the thermal oxide of a degeneratively doped Si substrate using chemical vapor deposition. (Alternatively, the network can be deposited onto the substrate from solution.) Iron nanoparticles deposited onto the substrate are used as catalysts for the growth. The growth is performed in a tube furnace between 700° and 900 °C using a gas such as ethylene as the source of carbon flowing in an argon/hydrogen carrier gas. The specific type of catalyst, method of deposition, carbon-containing vapor, and growth conditions do vary among research groups, and these details affect the density, uniformity and the average diameter of the SWNTs within the network. With care, networks with uniform sheet resistances between 10 and 100 k $\Omega$  per square can be grown across the surface of large-area wafers.

Following the growth, the networks are fabricated into devices using conventional microfabrication procedures. Contact electrodes (*e.g.* Ti/Au) are fabricated using photolithography and metal liftoff, and the unwanted network between devices is removed by masking the devices with photoresist and exposing the unprotected regions to an oxygen plasma etch.

A schematic of the device geometry that we use is shown in Fig. 2. The device structure is that of a field-effect transistor in

which the interdigitated electrodes form the source and drain, and the Si substrate and SiO<sub>2</sub> layer serve as the gate electrode and gate oxide, respectively. The conductance,  $G$ , is measured between the source and drain electrodes, and the substrate electrode forms a capacitive link,  $C$ , to the SWNT network. An applied substrate voltage,  $V_s$ , produces a charge,  $CV_s$ , on the network and is used to calibrate the charge effects from adsorbed molecules.

In addition to the conductance, sensors fabricated in the manner shown in Fig. 2 also provide a means of simultaneously measuring the network capacitance. The small capacitance of SWNTs,  $\sim 10^{-17}$  F, prohibits accurate measurement of individual SWNTs. However, the capacitance of a SWNT network with a typical density of 10 SWNTs  $\mu\text{m}^{-2}$  is about 10 nF  $\text{cm}^{-2}$ .<sup>5</sup> Thus, it is possible to construct compact sensors with  $C \sim 100$  pF, which can be measured with high precision.

## 3. Signal transduction

### Conductance-based detection

Kong, *et al.*<sup>1</sup> and Collins, *et al.*<sup>2</sup> were the first to establish that certain molecular adsorbates can significantly alter the electrical conductance of SWNTs. In such cases charge transfer between the adsorbate and the SWNT causes either an increase or a reduction in the number of mobile charge carriers. Kong, *et al.*<sup>1</sup> demonstrated that NH<sub>3</sub>, an electron donor, causes a reduction in the conductivity of p-type semiconducting SWNTs while NO<sub>2</sub>, an electron acceptor, causes an increase in conductance (Fig. 3).

In both cases the adsorbate binding energy is sufficiently large that the adsorbate remains attached to the SWNT long after the analyte is removed from the surrounding atmosphere. Typically, heat or ultraviolet light is required to desorb the analyte and return the SWNT to its initial conductance value.<sup>17</sup> This long desorption time causes the SWNT to act like a dosimeter integrating the dose of analyte. In this way, SWNTs can detect long-term exposure to extremely low doses of these gases, *e.g.* SWNT sensors coated with polyethylenimine (PEI), which enhances the sensitivity to NO<sub>2</sub>, respond in about 1000 s to concentrations as low as 100 part per trillion (see Fig. 4).<sup>4</sup>

Experiments indicate that NH<sub>3</sub> adsorbates donate approximately  $0.04 e^-$  per molecule,<sup>18</sup> while NO<sub>2</sub> binds to the SWNT

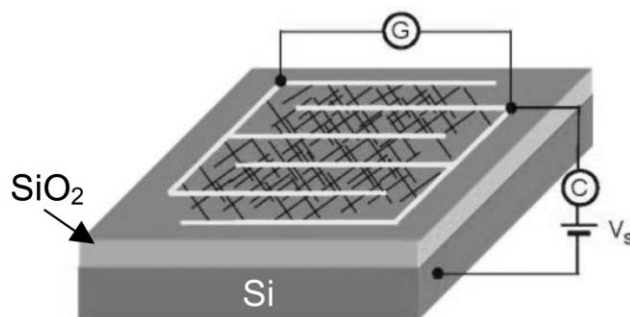


**Fig. 2** Schematic of a SWNT sensor. The SWNT network provides a conductive link between the interdigitated electrodes and a capacitive link to the conducting Si substrate.

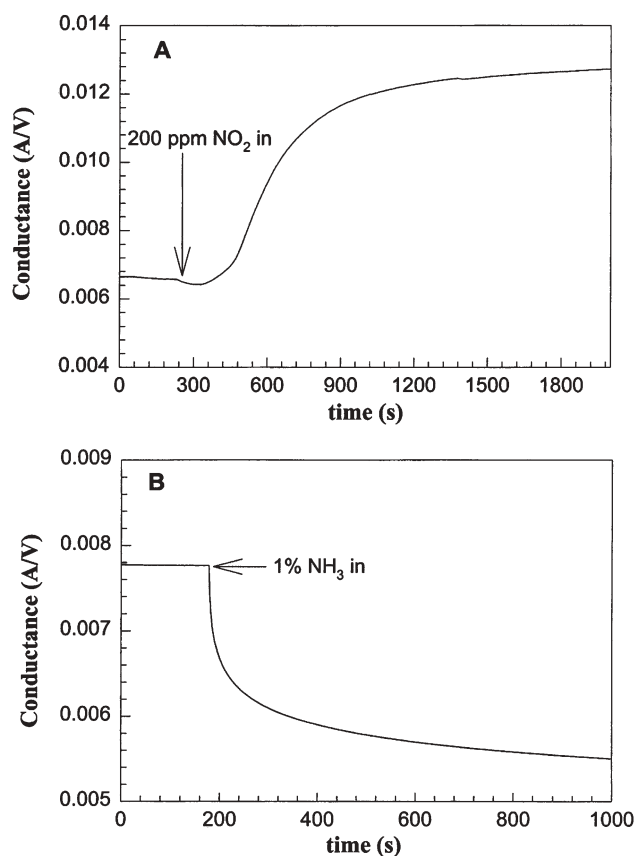


Fig. 3 Response of SWNTs to doses of NO<sub>2</sub> and NH<sub>3</sub>. (Reproduced with permission from Ref. 1. Copyright 2000 American Association for the Advancement of Science.)

surface with an energy of 0.8 eV and withdraws approximately 0.1 e<sup>-</sup> per molecule.<sup>4</sup> Numerical modeling indicates that the

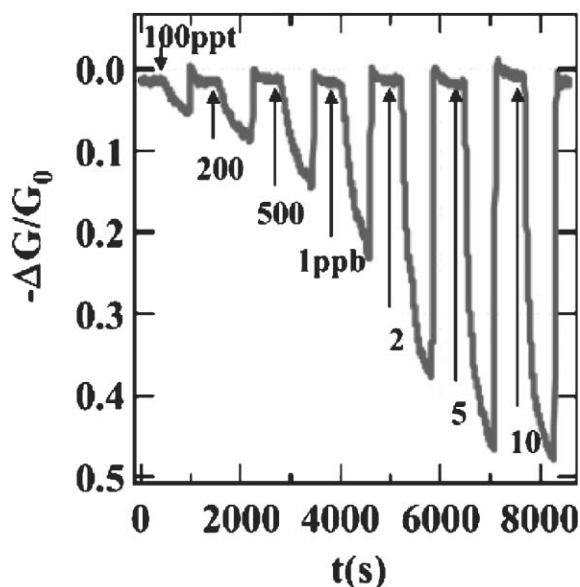


Fig. 4 Conductance response of a SWNT sensor to doses of NO<sub>2</sub> demonstrating 100-part-per-trillion sensitivity. The SWNTs were coated with PEI to enhance their sensitivity. The sensor was refreshed between doses by exposing it to ultraviolet light. (Reproduced with permission from Ref. 4. Copyright 2003 American Chemical Society.)

NO<sub>2</sub> molecular levels hybridize with the SWNT valence band resulting in the large binding energy and charge transfer.<sup>19</sup> However, these models predict a much smaller binding energy for NH<sub>3</sub>, which is in disagreement with experiment. Experimental evidence indicates that adsorbed water plays an important role in the NH<sub>3</sub>-SWNT interaction, a feature not taken into account in the theory.<sup>18</sup>

A list of calculated binding energies and the amount of charge transfer for several molecules is shown in Table 1.<sup>19</sup> Note that the theory predicts that both the binding energy and the amount of charge transfer can depend on the SWNT structure. It is also likely that defect sites either on the sidewalls or the open ends of the nanotubes are more reactive than the pristine sidewall and contribute significantly to the observed sensor response.

In order to experimentally explore the charge transfer effect with SWNTs, Star *et al.*<sup>20</sup> used monosubstituted benzenes to systematically vary the degree and sign of charge transfer. Each benzene derivative has a similar geometry in their noncovalent binding to the SWNTs, but the substituents provide different electron donating properties. As seen in Fig. 5, the amount of charge transfer (proportional to  $\Delta V_g$ ) varies linearly with the electron donating properties (indicated by the Hammett constant,  $\sigma_p$ ) of the molecule. This data is consistent with charge transfer as the origin of the conductance change.

One final note on conductance-based detection is that the presence of an analyte can also change the conductivity by modifying the charge-carrier mobility. Star, *et al.*<sup>8</sup> have used a mixture of PEI and starch polymers to produce a SWNT CO<sub>2</sub> sensor. In this case the CO<sub>2</sub> interacts with the PEI amino groups in the presence of water (from the hygroscopic starch) to produce carbamates, which has the net effect of introducing scattering centers that decrease the carrier mobility in the

Table 1 Calculated values of the binding energy and the charge transfer between various molecules and three types of SWNTs (data from Ref. 19)

	NO <sub>2</sub>	O <sub>2</sub>	H <sub>2</sub> O	NH <sub>3</sub>	CH <sub>4</sub>
(10,0) SWNT					
$E_a$ /meV	797	509	143	149	190
$Q/e$	-0.06	-0.13	0.04	0.03	0.03
(5,5) SWNT					
$E_a$ /meV	427	306	128	162	122
$Q/e$	-0.07	-0.14	0.03	0.03	0.02
(17,0) SWNT					
$E_a$ /meV	687	487	127	133	72
$Q/e$	-0.09	-0.1	0.03	0.03	0.03

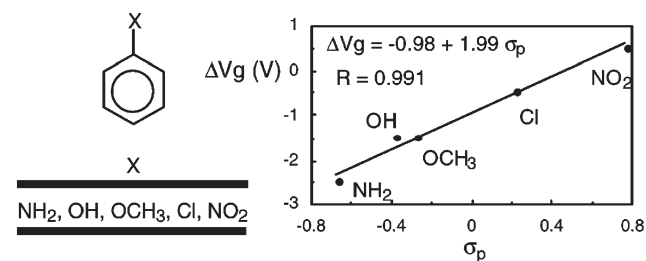


Fig. 5 Plot of the measured threshold shift (proportional to the amount of charge transfer) as a function of the Hammett constant,  $\sigma_p$ , of the benzene derivative. (Reproduced with permission from Ref. 20. Copyright 2003 American Chemical Society.)

SWNTs. Evidence for this reduced mobility is an observed decrease in the transconductance ( $dI/dV_g$ ) of the sensor, as opposed to the more commonly observed shift in threshold voltage that is evidence of charge transfer.

### Capacitance-based detection

While a few gases and vapors produce a strong conductance response in SWNTs, most gases and vapors weakly interact and produce only a small level of charge transfer. For these analytes an alternative transduction mode is desirable. Under an applied gate bias a large radial electric field emanates from the SWNT surface. This electric field polarizes molecular adsorbates on the SWNT surface, producing an increased capacitance. We have found that most polar molecules produce a strong capacitance response in SWNTs, and even non-polar polarizable molecules generate a finite response. This capacitance change provides a fast, sensitive, low-noise transduction mode to detect a wide range of weakly interacting chemical vapors.<sup>5</sup>

Fig. 6 shows the relative capacitance change,  $\Delta C/C_0$ , of a SWNT network measured in response to dilute, 0.5 s pulses of dimethyl methylphosphonate (DMMP), a simulant for the nerve agent sarin. The vapor pulses were delivered in dry air at a concentration,  $P$ , equal to 0.0005 of its equilibrium vapor pressure,  $P_0$ . Note that the capacitance response is rapid and recovers upon removal of the vapor. (In this case the response time is limited by the performance of the vapor delivery system.) Such a sensitive, rapid response and recovery is observed for a wide range of chemical vapors, and thus this transduction mechanism is an attractive candidate for constructing real-time chemical sensors for a variety of applications.

There are two possible states of the analytes observed in a capacitance measurement: condensed on the SWNT surface and in vapor phase in the high-field region in close proximity

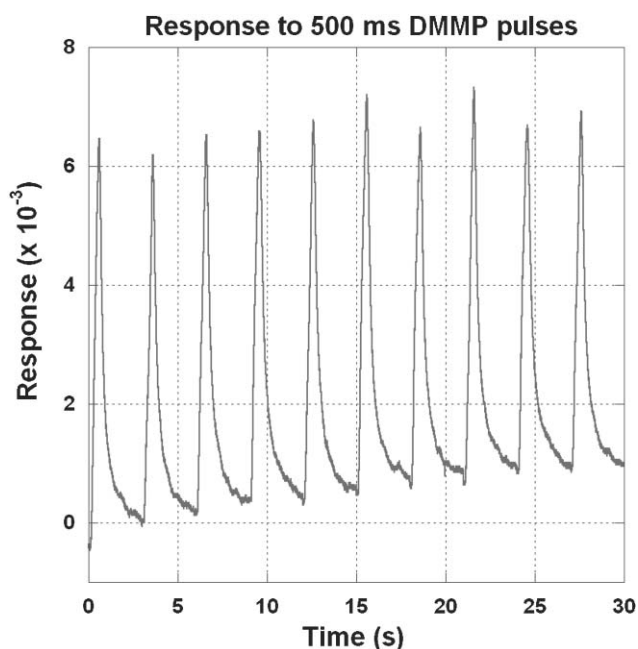


**Fig. 6** Capacitance response of a SWNT sensor to 500 ms pulses of DMMP delivered in air at  $P = 0.0005 P_0$ .

to the SWNTs. By studying the response to vapors with widely ranging values of  $P_0$ , we have concluded that the adsorbates dominate the capacitance response. The response from vapor phase molecules should scale as  $P\mu^2$  where  $\mu$  is the dipole moment.<sup>21</sup> We find that the relative response of two analytes with similar dipole moments and differing values of  $P_0$  correlates better with the ratio  $P/P_0$  than with the absolute concentration  $P$ . Such behavior is indicative of adsorbate molecules where  $P/P_0$  dictates the surface coverage.<sup>22</sup>

Two effects enhance the capacitance response of the adsorbates. First, the field strength is strongest at the SWNT surface and falls off rapidly in proportion to  $1/(r+r_0)$ , where  $r_0$  is the radius of the SWNT. Second, the density of adsorbates is much higher than the concentration in the vapor phase due to the attractive interaction with the surface. These two factors produce a surface-enhanced capacitance response that is much larger than the dielectric response of the vapor-phase molecules.

The adsorbate capacitance response can be attributed to field-induced polarization of surface dipoles.<sup>5</sup> Numerical simulations of acetone on SWNTs in the presence of an electric field indicate that for this molecule the dominant polarization effect is the modulation of the population of surface dipoles. The electric field alters the binding energy between the acetone and the surface resulting in a field-dependent population of adsorbates. Since the interaction with the SWNT surface preferentially orients the acetone, and correspondingly its dipole moment, the field controls the population of oriented surface dipoles. Additional contributions to the polarization include a field-dependent orientation of the intrinsic dipole moment and a field-induced polarization. The net result of these polarization effects is an easily measured increase in capacitance.

We observe a capacitance response to all of the chemical vapors we have tested, and further that these responses increase monotonically and smoothly with concentration over a wide range (see Fig. 7).<sup>23</sup> Note that both high vapor pressure analytes such as acetone ( $P_0 = 300$  parts per thousand) and low-vapor-pressure analytes such as the explosive simulant 2,4-dinitrotoluene ( $P_0 = 170$  parts per billion) produce comparable responses at a fixed value of  $P/P_0$ .

Over the range ( $P/P_0 = 0.0002$  to  $0.5$ ) and materials tested we consistently observe that the data can be fit by the expression  $\Delta C/C = \alpha(P/P_0)^n$  with values of  $\alpha$  ranging from 0.01 to 0.2 and  $n$  ranging from 0.4 to 1. The sensitivity for a particular molecule is determined by the interaction with the SWNTs, the intrinsic molecular dipole moment, and preferred orientation of the adsorbate dipole on the SWNT surface.

Also shown in Fig. 7 is a conservative estimate of our minimum detectable capacitance change,  $\Delta C/C = 10^{-4}$ . Due to the sublinear scaling of many analytes, *i.e.*  $n < 1$ , extrapolation of our data to the minimum detectable  $\Delta C/C$  produces impressive detection limits (sub-part-per-billion levels for both for the nerve agent simulant, DMMP, and the explosive simulant, 2,4-dinitrotoluene), and large dynamic ranges. Currently, validation of this scaling to low concentrations awaits future testing.

The capability to detect such low concentrations is an area where SWNT sensors offer an advantage over conventional

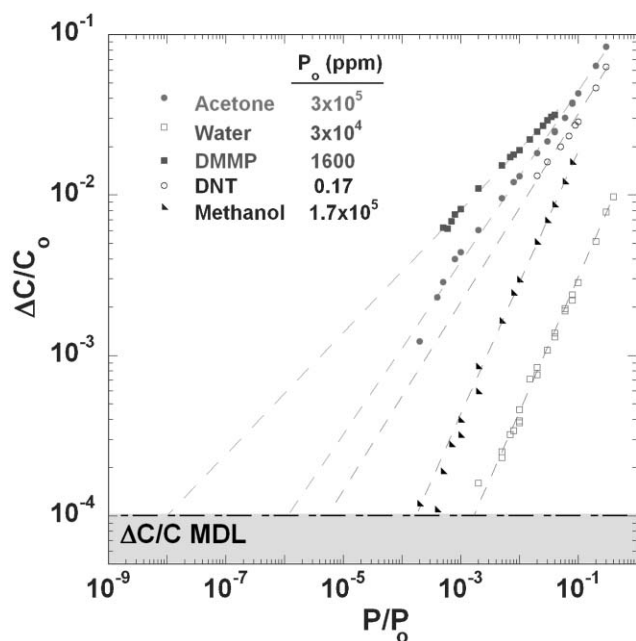


**Fig. 7** Capacitance response as a function of analyte concentration for different analytes. Each data set is well fit by the expression  $\Delta C/C = \alpha(P/P_0)^n$ , with  $n$  ranging from 0.4 to 1 and  $\alpha$  ranging from 0.01 to 0.2.  $P_0$  at room temperature for each analyte is listed in units of ppm.

solid-state sensor technology. Such conventional sensors operate by detecting the loading of a sensor material with analyte. However, at low concentrations ( $\sim 1$  part per billion) there are insufficient vapor molecules to load the active material to detectable levels. In order to achieve part-per-billion detection levels a highly surface-sensitive detection mechanism is required. SWNT sensors provide this unique capability.

It should be noted that the results shown in Figs. 6 and 7 were obtained by diluting saturated analyte vapors with dry air. Similar results are obtained by diluting the vapors with humid air, with some moderate changes in sensitivity ( $< 2$ ). The absence of a large humidity effect can be attributed to the weak interaction between water molecules and SWNTs.

In addition to the dielectric effects described above, charge transfer from the adsorbed analyte also affects the SWNT capacitance, although to a lesser degree. The SWNT capacitance can be modeled as two capacitors in series,  $C = (1/C_G + 1/C_Q)^{-1}$  where  $C_G$  is the gate capacitance, a function of the oxide dielectric and the dielectric effects of the adsorbates, and  $C_Q$  is the quantum capacitance, a function of the SWNT Fermi energy,  $E_F$ .<sup>24</sup> At zero temperature,  $C_Q = e^2 g(E_F)$  where  $g(E)$  is the SWNT network density of states (for finite temperature thermal broadening effects have to be taken into effect to calculate  $C_Q$ <sup>25</sup>). Adsorbate charge transfer can shift  $E_F$  into a region with a different density of states resulting in a change in  $C_Q$ . At  $V_s = 0$ , typical values of  $C_Q$  and  $C_G$  are approximately  $100 \text{ aF } \mu\text{m}^{-1}$  and  $10 \text{ aF } \mu\text{m}^{-1}$ , respectively. Consequently,  $C_Q$  constitutes only about 10% of the measured sensor capacitance, which results in a small, but measurable charge response.

The charge sensitivity of  $C$  and  $G$  can be determined empirically by measuring  $C(V_s)$  and  $G(V_s)$ , and using  $Q = CV_s$ .

Typical data for our sensors is shown in Fig. 8 where the substrate bias was swept from  $-0.9 \text{ V}$  to  $+0.9 \text{ V}$ . The slope of each curve is a measure of the charge sensitivity. Typically we find at  $V_s = 0$  that  $1/G_0 \text{ d}G/\text{d}Q$  is about ten times larger than  $1/C_0 \text{ d}C/\text{d}Q$ . Consequently, a given charge,  $Q$ , will produce about an order of magnitude larger value of  $\Delta G/G_0$  than  $\Delta C/C_0$ .

The capacitance response contains contributions from both the dielectric and the charge effects of the analyte, *i.e.*  $\Delta C = \frac{\partial C}{\partial \epsilon} \Delta \epsilon + \frac{\partial C}{\partial Q} \Delta Q$  where the second term arises from the charge transfer response *via*  $C_Q$ . We have used simultaneous capacitance and conductance measurements to quantitatively determine the relative contributions of the charge and dielectric response.<sup>10</sup> For most vapors we observe that the charge contribution to the capacitance response is  $\sim 10\%$  of the total  $\Delta C$ . One exception is  $\text{NH}_3$ , where a large charge transfer,  $\Delta C_Q$ , dominates the capacitance response.

### Comparison of $C$ and $G$ sensing

For both capacitance and conductance detection the dominant physical mechanism behind sensitivity to ambient is adsorption of species on the surface of the nanotubes. Surface coverage by adsorbed species is related not to the concentration of species in the ambient (*i.e.*, the partial pressure  $P$ ), but rather to the fraction,  $P/P_0$ , of the equilibrium vapor pressure  $P_0$ . In other words, SWNT sensors respond to analytes not according to their local abundance ( $P$ ) but according to their likelihood of condensing on a surface ( $P/P_0$ ). As a result the sensors respond equally well to both high- and low-vapor-pressure analytes. Since the low vapor pressure of many materials of interest, such as nerve agents, blister agents, and explosives, has made their detection by conventional sensors a challenge, this indicates an area where SWNT sensors offer unique capabilities.

In choosing the best transduction mode, the conductance response is better for those analytes that produce a large charge transfer. For weaker interacting vapors and gases the capacitance detection mode offers several advantages, such as higher sensitivity, lower noise, larger dynamic range and better recovery. Simultaneous capacitance and conductance

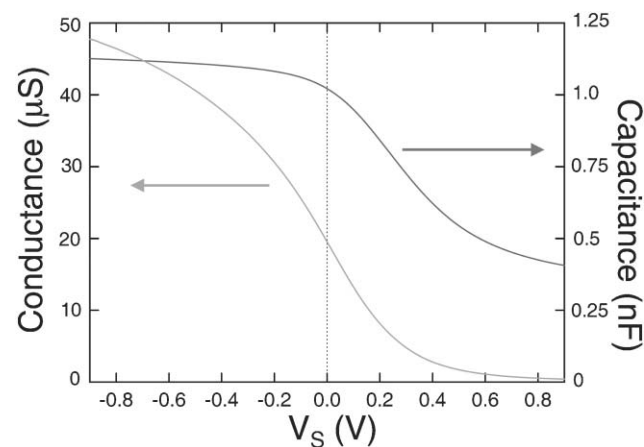


**Fig. 8** Dependence of the network capacitance and conductance on substrate bias,  $V_s$ . The slopes at  $V_s = 0$  are a measure of the charge sensitivity.

measurements can be made in the same sensor. In fact, at low to moderate analyte concentrations the ratio,  $\Delta G/\Delta C$ , produces a concentration-independent intrinsic parameter characteristic of the vapor.<sup>10</sup>

While conductance-based SWNT sensors are generally well behaved at low vapor concentration, several undesirable properties are observed at high concentrations. Such properties include partial recovery following exposure and saturation effects that limit the dynamic range of the sensor. We find that these and other such effects are limited to the charge response and thus affect conductance detection to a much greater extent than capacitance detection.

The effects of saturation are shown in Fig. 9, which shows the capacitance and the conductance response measured simultaneously in the same sensor to varying concentrations of acetone. The conductance response saturates at about 1%  $P_0$ . This saturation indicates that the active surface sites of the SWNT are fully populated with acetone and that additional adsorption of acetone does not contribute additional charge transfer.

In contrast, the capacitance response continues to increase above 1%  $P_0$  with no observable saturation. Evidently, there are either additional adsorption sites available that do not contribute charge transfer or the surface electric field extends beyond the first monolayer of acetone and is able to polarize additional molecular layers. In either case, the capacitance response provides an accurate measure of the vapor concentration over the full range of concentrations. This lack of saturation is consistently observed for many vapors as is shown in Fig. 7. Thus, capacitance detection offers improved dynamic range over conductance detection and provides both lower minimum detectable levels and an absence of saturation at high concentrations.

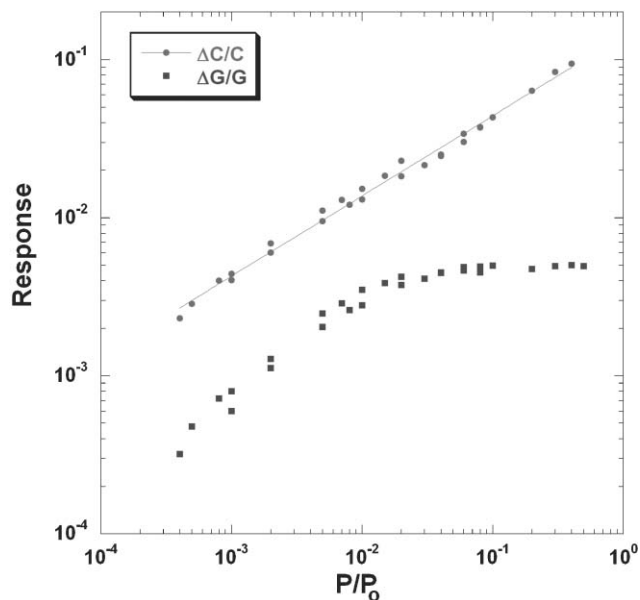


**Fig. 9** Magnitude of the conductance and capacitance response as a function of acetone concentration. The conductance response saturates at about 0.01  $P_0$ , while the capacitance response continuously increases.

## 4. Electrical noise

### Conductance noise

For detecting dilute concentrations of chemical vapors the minimum detectable level is established by the ratio of the signal to the background noise. Thus, the noise is a critical parameter for detecting trace amounts of chemical vapors. Of particular importance is low-frequency noise, since chemical detection is typically performed at frequencies  $<10$  Hz.

Unfortunately SWNTs generate a high level of low-frequency  $1/f$  noise, so called because the noise power density decreases inversely with the measurement frequency. This noise is present in almost all electronic systems. In many bulk electronic materials the  $1/f$  component of the noise power density,  $S_V(f)$ , is empirically found to obey the relationship,  $S_V(f) = \alpha_H/N V^2/f$ ,<sup>26</sup> where  $V$  is the applied voltage,  $N$  is the number of charge carriers in the system and  $\alpha_H$  is the Hooge parameter, which for many materials is  $\sim 10^{-3}$ .<sup>27</sup> Because SWNTs contain such a small number of charge carriers, their level of  $1/f$  noise is quite high. Consequently, conductance-based sensors that contain just one or a few SWNTs produce a high level of  $1/f$  noise reducing the signal-to-noise ratio.

SWNT networks provide one solution to this problem. By constructing devices that contain millions of SWNTs (and thus a large value of  $N$ ) the  $1/f$  noise, and correspondingly the minimum detectable level, can be significantly improved. We have studied the noise behavior of SWNT network devices with sizes ranging from  $10^{-7}$  to  $1$  cm<sup>2</sup> with varying network densities, and we have found an empirical relationship that can be used to predict the  $1/f$  noise performance of network sensors. We find that  $S_V(f) = 9 \times 10^{-11} R/L^{1.3} V^2/f$  where  $R$  is the device resistance in Ohms and  $L$  is the spacing between the electrodes in  $\mu\text{m}$ .<sup>12</sup> The data used to establish this formula are found in Fig. 10. (Since the noise scales as  $1/N$ , we expect that the noise should scale as  $R/L^2$  instead of  $R/L^{1.3}$ . However, we often observe non-ideal geometric scaling of the device resistance,<sup>9</sup> which most likely accounts for the non-ideal scaling of the noise.)

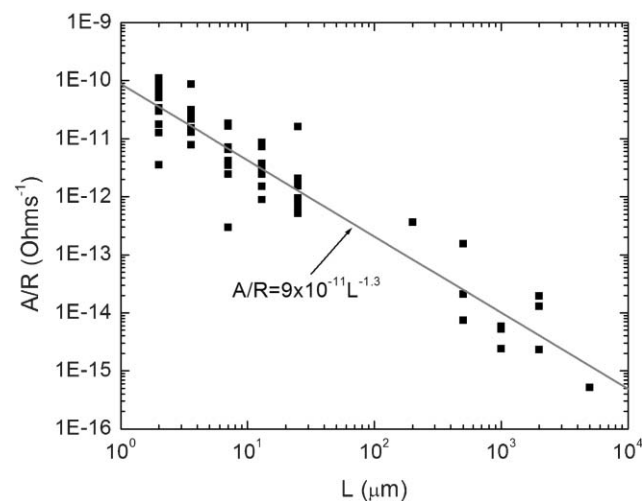


**Fig. 10** Amplitude of  $1/f$  noise in SWNT networks divided by the device resistance measured for devices with electrode spacings ranging from 2 to 5000  $\mu\text{m}$ .

We have used this formula to establish our sensor design, which consists of large-area (0.25 to 4 mm<sup>2</sup>) sensors with interdigitated electrodes for low-resistance. By measuring the device capacitance and the minimum detectable change in substrate voltage (as limited by the conductance noise), we can estimate the minimum charge sensitivity of our conductance measurements by using the relationship  $\Delta Q = C\Delta V_s$ . From this measurement and the average SWNT network density, we establish that our minimum charge sensitivity is  $\sim 0.01 e^-$  per SWNT. Thus, for adsorbates that produce this level of charge transfer, the sensors provide single molecule per SWNT sensitivity.

### Capacitance noise

Unlike resistors, conventional capacitors do not produce electrical noise. However, there is a source of 1/f noise in the SWNT capacitance sensors. As discussed above, the SWNT capacitance can be treated as the series combination of the geometric capacitance and the quantum capacitance. Because  $C_Q$  is sensitive to charge, the same charge fluctuations that produce conductance noise will introduce fluctuations in the total measured capacitance. However, as detailed above the capacitance is much less sensitive to charge than the conductance, so the level of 1/f noise is proportionally reduced.

## 5. Chemical specificity

In order for a chemical sensor to be effective, it must be able to discriminate and identify targets of interest from among a mixture. This is a difficult problem as the environments of interest may include volatile organic background materials, and among all the constituents, the specific “target” may be extremely dilute.

One solution that has been shown very effective is described as the “electronic nose”.<sup>28</sup> A parallel array of differently modified transducers is configured so as to be exposed uniformly to the flowing air stream. Proven designs include thin films (typically polymers) on mass-sensitive resonant frequency sensors<sup>29</sup> between small metal electrodes,<sup>30</sup> or with

dispersed conductive particles,<sup>31</sup> and transduction in these cases involves measuring mass changes (frequency shifts), capacitance changes, or conductivity changes, respectively. These changes are induced by sorption of analyte in the polymer, and reflect changes in the mass or volume of the film. Sorption efficiency is in turn governed by certain physicochemical and complementary properties of the film and analyte: polarizability, dipolarity, effective hydrogen bond acidity, effective hydrogen bond basicity, and dispersion/cavity formation efficacy.<sup>29</sup> The thin film materials are selected based on the extent to which they at least approximate an orthogonal basis set of measurements. Generally this is accomplished by using three to six discretely sensitized sensors. Optimal film selection thus effectively spans a five dimensional space, and analyte identification involves pattern recognition of responses within this space.<sup>32</sup> Three-component mixtures, however, are still problematic.<sup>33</sup>

SWNT sensors can make a significant difference here, as measurements of  $\Delta C$  and  $\Delta G$  are sensitive to dipole moment and polarizability of the adsorbate–SWNT couple, and charge transfer between the adsorbate and the SWNT. This adds two further orthogonal dimensions to the space spanned by a sensor array, suggesting a substantial improvement in resolution and sensitivity.

Although unmodified SWNT sensors clearly have a role to play in multi-sensor array systems, it is worth investigating whether it is possible to utilize chemoselective coatings in a fashion similar to other transducers. We begin by application of thin films of some of the special sorbent polymers which have found use in nose sensors: HC (a hyperbranched hexafluoro-carbo-silane),<sup>34</sup> PIB (polyisobutylene), and NMA (a hyperbranched naphthyl hexafluoropropanol allyl), as well as two others, PMMA (poly(methylmethacrylate)), and PDMS (poly(dimethylsiloxane)). Devices were covered with thin films (<100 nm) of each of these materials, and the effect on capacitance and conductance response was observed for a standard set of analytes (Fig. 11).

Although both selective amplification and filtering effects are observed, the response profile does not reflect the sorption

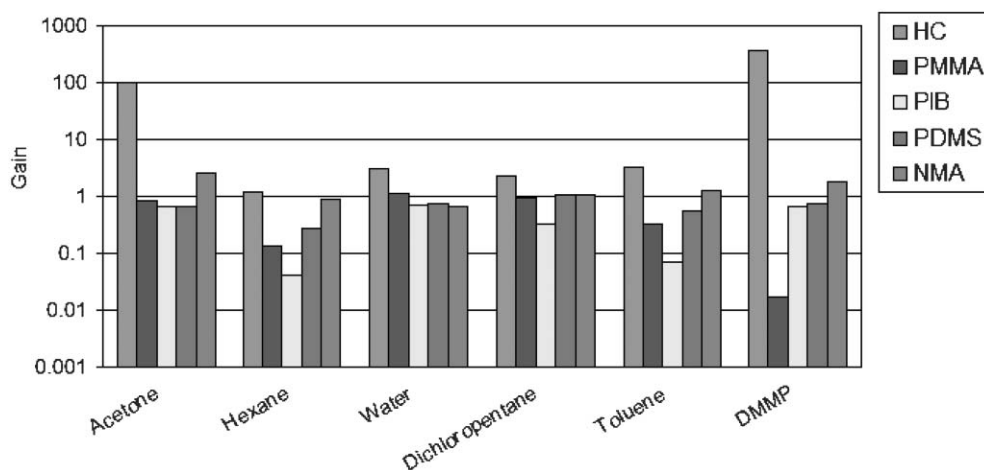


**Fig. 11** Ratio of the capacitance response of polymer-coated sensors to the response of an uncoated sensor for different vapors. The vapors were delivered at 0.01  $P_0$  except for DMMP which was delivered at 0.001  $P_0$ .

properties of the polymers themselves. For example, NMA and PIB, two polymers used in nose arrays, have very little effect on the sensor response despite their sorption properties. This surprising result may be attributed to the highly surface specific nature of the SWNT capacitance and conductance responses. In order to be “sensed” by the device, the analyte must be free to form a low energy configuration with the SWNT, and the films tend to interfere with that. Further, while the sorbent polymers certainly concentrate the target analyte in the vicinity of the SWNT, it is only analyte species literally at the surface that interact with and modify the electronic properties of the SWNT. For this reason we are now investigating the effect of smaller molecules attached directly to the SWNT surface. This work is very preliminary at this point, and will not be discussed here.

We envision that the most versatile implementation of a SWNT sensor technology will be its eventual use as the sensor element in a micro gas analyzer. In such a system a front-end vapor delivery system is used to create a short pulse of target analyte that is temporally separated from interferents.<sup>35</sup> The rapid response time and high sensitivity of SWNT sensors is well suited for such temporal-based discrimination techniques.

The temporal separation is achieved by using a micro-machined preconcentrator upstream of a micro gas chromatograph. The preconcentrator consists of a selectively sorbent polymer covering a metal grid, appropriately configured for rapid thermal cycling. Targeted materials preferentially accumulate in the preconcentrator. A thermal pulse is generated to cause a sudden out-gassing of all condensed material in as little as 10 milliseconds and on a cycle of a few (1–100) seconds. Entraining this to flow into a micro gas chromatograph will disperse the target analyte from interferents before it arrives at the sensor element. In this case the rapid response time of SWNT sensors can be used to temporally distinguish the response of a target analyte. Such a system, customized for SWNT sensors, is currently under development.

## 6. Summary

SWNT sensors offer great promise for compact, low-power chemical detectors. The capability now exists to inexpensively manufacture low-noise SWNT sensors with high yield, and efforts are now underway to design sensors for particular applications. In this stage of development it is important to consider those areas where SWNT sensors offer an advantage over conventional sensor technologies.

One potential area is trace detection of certain chemical warfare agents and explosives for defence and homeland security applications. These materials require the detection of extremely low concentrations of the target analyte. For both capacitance and conductance detection the dominant physical mechanism behind sensitivity to ambient is adsorption of species on the surface of the nanotubes. Surface coverage by adsorbed species is related to the fraction,  $P/P_0$ , of the equilibrium vapor pressure. As a result the SWNT sensors respond well to low-vapor-pressure analytes. Since the low vapor pressure of many materials of interest, such as nerve agents, blister agents, and explosives, has made their detection

by conventional sensors a challenge, this indicates an area where SWNT sensors offer unique capabilities.

## References

- 1 J. Kong, N. R. Franklin, C. Zhou, M. G. Chapline, S. Peng, K. Cho and H. Dai, *Science*, 2000, **287**, 622.
- 2 P. G. Collins, K. Bradley, M. Ishigami and A. Zettl, *Science*, 2000, **287**, 1801.
- 3 A. Javey, J. Guo, Q. Wang, M. Lundstrom and H. Dai, *Nature*, 2003, **424**, 654.
- 4 P. Qi, O. Vermesh, M. Grecu, A. Javey, Q. Wang, H. Dai, S. Peng and K. Cho, *Nano Lett.*, 2003, **3**, 347.
- 5 E. S. Snow, F. K. Perkins, E. J. Houser, S. C. Badescu and T. L. Reinecke, *Science*, 2005, **307**, 1942.
- 6 C. Staii and A. T. Johnson, *Nano Lett.*, 2005, **5**, 1774.
- 7 J. P. Novak, E. S. Snow, E. J. Houser, D. Park, J. L. Stepnowski and R. A. McGill, *Appl. Phys. Lett.*, 2003, **83**, 4026.
- 8 A. Star, T.-R. Han, V. Joshi, J.-C. P. Gabriel and G. Gruner, *Adv. Mater.*, 2004, **16**, 2049.
- 9 E. S. Snow, J. P. Novak, P. M. Campbell and D. Park, *Appl. Phys. Lett.*, 2003, **82**, 2145.
- 10 E. S. Snow and F. K. Perkins, *Nano Lett.*, 2005, **5**, 2414.
- 11 P. G. Collins, M. S. Fuhrer and A. Zettl, *Appl. Phys. Lett.*, 2000, **76**, 894.
- 12 E. S. Snow, J. P. Novak, M. D. Lay and F. K. Perkins, *Appl. Phys. Lett.*, 2004, **85**, 4172.
- 13 M. Dresselhaus, G. Dresselhaus and Ph. Avouris, *Carbon Nanotubes: Synthesis, Structure, Properties and Applications*, Springer-Verlag, Berlin, 2001.
- 14 T. Hertel, R. E. Walkup and P. Avouris, *Phys. Rev. B: Condens. Matter Mater. Phys.*, 1998, **58**, 13870.
- 15 M. M. J. Treacy, T. W. Ebbesen and J. M. Gibson, *Nature*, 1996, **381**, 678.
- 16 M. S. Fuhrer, J. Nygard, L. Shih, M. Forero, Y. G. Yoon, M. S. C. Mazzoni, H. J. Choi, J. Ihm, S. G. Louie, A. Zettl and P. L. McEuen, *Science*, 2000, **288**, 494.
- 17 R. J. Chen, N. R. Franklin, J. Kong, J. Cao, T. W. Tomblor, Y. Zhang and H. Dai, *Appl. Phys. Lett.*, 2001, **79**, 2258.
- 18 K. Bradley, J.-C. P. Gabriel, M. Briman, A. Star and G. Gruner, *Phys. Rev. Lett.*, 2003, **91**, 218301.
- 19 J. Zhao, A. Buldum, H. Han and J. P. Lu, *Nanotechnology*, 2002, **13**, 195.
- 20 A. Star, T.-R. Han, J.-C. P. Gabriel, K. Bradley and G. Gruner, *Nano Lett.*, 2003, **3**, 1421.
- 21 J. D. Jackson, in *Classical Electrodynamics*, Wiley, New York, 2nd edn., 1975, ch. 4, pp. 155–158.
- 22 S. Brunauer, P. H. Emmett and E. Teller, *J. Am. Chem. Soc.*, 1938, **60**, 309.
- 23 J. A. Robinson, E. S. Snow and F. K. Perkins, *Sens. Actuators A* submitted.
- 24 S. Rosenblatt, Y. Yaish, J. Park, J. Gore, V. Sazonova and P. L. McEuen, *Nano Lett.*, 2002, **2**, 869.
- 25 J. Guo, S. Goasguen, M. Lundstrom and S. Datta, *Appl. Phys. Lett.*, 2002, **81**, 1486.
- 26 F. N. Hooge, *Phys. Lett.*, 1969, **29A**, 139.
- 27 F. N. Hooge, *IEEE Trans. Electron Devices*, 1994, **41**, 1926.
- 28 *Sensors and Sensory Systems for an Electronic Nose*, NATO Science Series E, ed. by J. Gardner and P. N. Bartlett, Springer, New York, 1992.
- 29 J. W. Grate, *Chem. Rev.*, 2000, **100**, 2627.
- 30 S. V. Patel, T. E. Mlsna, B. Fruhberger, E. Klaassen, S. Cemalovic and D. R. Baselt, *Sens. Actuators, B*, 2003, **96**, 541.
- 31 M. C. Lonergan, E. J. Severin, B. J. Doleman, S. A. Beaber, R. H. Grubbs and N. S. Lewis, *Chem. Mater.*, 1996, **8**, 2298.
- 32 R. E. Shaffer, S. L. Rose-Pehrsson and R. A. McGill, *Anal. Chim. Acta*, 1999, **384**, 305.
- 33 M.-D. Hsieh and E. T. Zellers, *Anal. Chem.*, 2004, **76**, 1885.
- 34 E. J. Houser, D. L. Simonson, J. L. Stepnowski and R. A. McGill, *Polym. Mater. Sci. Eng. Preprints*, 2003, **88**, 548.
- 35 W. C. Tian, S. W. Pang, C. J. Lu and E. T. Zellers, *J. Microelectromech. Syst.*, 2003, **12**, 264.